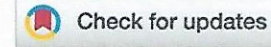
Polymer Chemistry



COMMUNICATION

View Article Online



Cite this: DOI: 10.1039/d0py00016g

Received 4th January 2020, Accepted 25th February 2020 DOI: 10.1039/d0py00016g

rsc.li/polymers

Self-healing behaviour of furan-maleimide poly(ionic liquid) covalent adaptable networks†

Katelyn M. Lindenmeyer, R. Daniel Johnson o and Kevin M. Miller *

Poly(ionic liquid) covalently adaptable networks containing thermoreversible furan—maleimide linkages were prepared and characterized for their thermal, mechanical and conductive properties. Self-healing behaviour was initially evaluated using oscillatory rheology where a *G'/G"* crossover temperature of ~110 °C was observed. Anhydrous conductivities, as determined by dielectric relaxation spectroscopy, were found to be on the order of 10⁻⁸ S cm⁻¹ at 30 °C. Recovery of >70% of the original stress and strain at break was found within 2 hours at 105 °C as determined from tensile testing experiments, with breakage occurring at a new point on the film. Recovery of conductivity was completed utilizing chronoamperometric cycling whereby >75% of the original current was recovered within two hours at 110 °C.

Introduction

Covalently-crosslinked networks or thermosets are well known for their mechanical superiority (high fracture strength, moduli, *etc.*) and, as a result, are utilized in a wide range of applications ranging from composites to coatings; however, the application of high stress to these thermosetting materials can result in permanent deformation (abrasions, cracks, fractures, *etc.*). Recently, the purposeful inclusion of dynamic covalent chemistry (DCC) into network thermosets has allowed for covalent bond reshuffling upon the application of strain, thereby healing damages. Alternatively, many dynamic bonds can be chemically activated by a number of external stimuli such as heat, light or pH. Examples of DCCs are numerous, including disulphide bond exchange, Alternatively, many dynamic esters and thiol-Michael bonds. Petworks that exhibit such reversible rearrangements are referred to as covalent

adaptable networks (CANs), the history and applications of which have been reviewed. 10-14

One DCC that has been utilized frequently in CANs is the 'click-like' Diels-Alder (DA) cycloaddition, in particular the cycloadduct formed between maleimide and furan, as the reaction can be conducted (forward or reverse) at opportune temperatures. 15-17 While the origin of this thermally reversible cycloaddition dates back to Craven's patent in 1969,18 Wudl et al. utilized this chemistry specifically in networks prepared from multi-functional furan and maleimide monomers. Healing efficiencies of approximately 50% were observed when damaged samples were heated to 120 °C.19 Bowman and coworkers further demonstrated the reversibility of the furanmaleimide linkage through small molecule kinetic studies and network rheology.15 A crossover temperature (Tcrossover) of 92 °C was observed, specific to their system, whereby the network behaved more like an elastic solid below $T_{
m crossover}$ but acted as a liquid-like sol above Tcrossover. Ultimately, the dynamic nature of the furan-maleimide linkage, coupled with the control at which the bond can be thermally activated, could be manipulated to achieve rehealing of small cracks and abrasions or even recycling. A number of exciting new materials and applications for furan-maleimide-based CANs have been explored, examples of which include organicinorganic interpenetrating polymer networks (IPN),20 shapememory materials,21 3D printing22 and melt-blown fibers.23

Poly(ionic liquid)s or polymerized ionic liquids (PILs) are polymers synthesized with an ionic liquid (IL) group (or groups) covalently incorporated into the repeating unit (polymer backbone or side chain). PILs have attracted a great deal of interest in applications such as electroactive devices, smart materials and gas separation membranes. PILs are capable of retaining a number of the attractive properties of their ionic liquid precursors (thermal and chemical stability, high ionic conductivity, wide electrochemical window) while gaining mechanical strength and stability through the covalent incorporation of the IL group into various macromolecular architectures. PILs are polymers.

Department of Chemistry, Murray State University, Murray, KY, 42071, USA. E-mail: kmiller38@murraystate.edu

 $\dagger Electronic$ supplementary information (ESI) available. See DOI: 10.1039/d0py00016g

transport in PILs is affected by the glass transition temperature $(T_{\rm g})$, molecular weight, water content and the chemistry and morphology of the polymer and ionic liquid group. For example, an increase in ionic conductivity is often observed with a decrease in $T_{\rm g}$. Bulky counteranions such as bis(trifluoromethanesulfonyl)imide [NTf₂] provide extra free volume to enhance the segmental motion of the polymer, thereby increasing the transference of ions and thus ionic conductivity. 37,38

PILs that contain the imidazolium cation have received the most attention, presumably due to the ease at which the two heterocyclic nitrogens can be differentially functionalized. The vast majority of imidazolium-based PILs stem from the polymerization of vinyl-, styrenyl- or (meth)acrylic-functionalized imidazole or imidazolium monomers;24-28,39-44 however, several research groups have also incorporated imidazolium groups into step-growth architectures such as polyesters⁴⁵ and polyurethanes36 and covalently crosslinked PILs.46-49 Rehealing in PILs is relatively new. Several reports for non-CAN PILs have relied on the intrinsic rearrangement of ion pairing across a crack to facilitate rehealing. 50,51 Drockenmuller was one of the first to tackle the idea of CAN PILs with a series of vitrimeric 1,2,3-triazoium PILs where dynamic S_N2 transalkylation reactions were activated at high temperatures (>100 °C).52,53 Konkolewicz demonstrated an improvement in this dynamic transalkylation chemistry where a quaternary anilinium system was activated at only 60 °C while maintaining mechanical stability under ambient conditions.⁵⁴ Evans more recently described the rehealing ability of PIL CANs which utilized boronic ester linkages.⁵⁵ PIL networks which were purposefully cut were found to recover >95% of the original conductivity in just 10 minutes with the addition of pressure.

In this Communication, the synthesis and self-healing behaviour of two imidazolium-containing PIL CANs is disclosed. Thermoreversible furan-maleimide linkages were utilized to induce recovery of mechanical and conductive properties upon exposure to elevated temperature. Within 2 hours at 105 °C, recovery of >70% of mechanical properties, as determined from DMA tensile testing, was observed with up to 90% recovery observed after slightly longer periods of time. Rehealed samples were also found to fracture at a new point, away from the reseal. Furthermore, the conductivity of a sample placed between two planar copper electrodes was found to recover to >75% in 2 hours at 110 °C after the sample was completely severed between the electrodes with a razor blade.

Results and discussion

Imidazolium-containing maleimide monomers were prepared as shown in Scheme 1. Furan-protected N-(4-bromobutyl)maleimide 1 ⁵⁶ was coupled with sodium imidazole⁵⁷ to produce furan-protected N-(4-imidazoyl)maleimide 2. After addition of another mole of 1, followed by anion exchange with LiNTf₂, furan-protected imidazolium bromide salt 3 was isolated. Deprotection of the furan at 120 °C led to the targeted imidazolium-containing, maleimide [NTf₂] monomer 4. To prepare the bisimidazolium maleimide [NTf₂] monomer, 1,6-bisimidazoylhexane⁵⁷ was reacted with two moles of furan-protected N-(4-bromobutyl)maleimide 1, resulting in the bisimidazolium bromide salt, which underwent subsequent anion-exchange to bisimidazolium NTf₂ salt 5 after reaction with LiNTf₂. Furan deprotection occurred as before, resulting in the targeted monomer 6.

Synthesis of the PIL CANs was conducted by first dissolving maleimide-terminated IL monomer 4 or 6 with the trifuran-functionalized crosslinker TMPT-FUR, prepared from trimethyloyl propane triacrylate and furfuryl mercaptan,²² in acetonitrile (1:1 ratio of furan: maleimide functional groups).

Scheme 1

The solution was poured into a custom mold, made with a Teflon™ outer ring and a glass bottom, held together with binder clips. The solution was placed into a convection oven at 120 °C until solid film formation was observed (45–50 minutes). The cured sample was then placed in a vacuum oven (50 °C, <0.1 mm Hg) for 12 hours in ensure complete solvent removal. Polymer thickness was found to be 250–300 µm. Complete functional group conversion was confirmed by FT-IR spectroscopy (Fig. S15 and S16†) through the disappearance of the maleimide (695 and 828 cm⁻¹)⁵⁸ signals and Soxhlet extraction of the networks in acetonitrile indicated >98% gel fraction. Analysis of the soluble fraction by FTIR also did not indicate any unreacted maleimide groups present. Elemental analysis was also employed to confirm composition (Table S1†).

Oscillatory rheology was conducted initially to explore the ability of the PIL networks to flow under various relaxation conditions. A strain of 0.5% was chosen based upon LVR (linear viscoelastic region) measurements and storage (G') and loss (G'') moduli were monitored as a function of frequency at various temperatures (Fig. 1). As has been demonstrated pre-

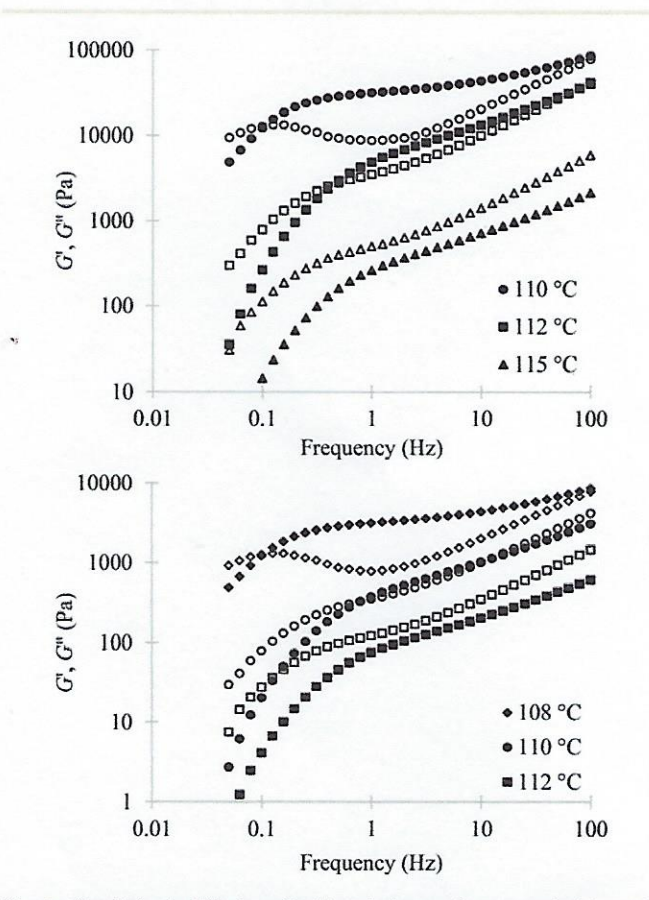


Fig. 1 (Top) Elastic (filled symbols) and viscous (open symbols) moduli versus frequency for PIL-CAN-IM at temperatures above (115 °C), near (112 °C) or below (110 °C) $T_{\rm crossover}$. (Bottom) Analogous plot for PIL-CAN-IM2 at temperatures above (112 °C), near (110 °C) or below (108 °C) $T_{\rm crossover}$. Additional data can be found in the ESI (Fig. S21 and S22†).

viously for Diels–Alder CANs and several other thermoreversible networks, there exists a characteristic temperature $T_{\rm crossover}$ (the temperature where G' and G'' are equal), where the network is more solid-like when $T < T_{\rm crossover}$ but acts more like a fluid-like sol when $T > T_{\rm crossover}$. At temperatures slightly below $T_{\rm crossover}$, the dynamic reaction at lower frequencies is greater than the rate of bulk deformation and the material begins to act more fluid-like. Both PIL-CANs examined here exhibited $T_{\rm crossover}$ values at approximately 110 °C (PIL-CAN-IM at 112 °C and PIL-CAN-IM2 at 110 °C with an experimental error of ± 3 °C). As will be discussed shortly, temperatures at or below $T_{\rm crossover}$ were chosen to test the rehealability of these networks in terms of the mechanical and conductive properties. Both polymers visually reverted to a liquid state at temperatures above 125 °C.

Prior to testing the rehealability of these networks, thermal properties were determined for each PIL-CAN. Glass transition temperatures (T_g) were determined by differential scanning calorimetry (DSC), the results of which are shown in Table 1. The PIL-CAN-IM system exhibited a higher T_{σ} (12.8 °C) than PIL-CAN-IM2 (2.8 °C), presumably due to a higher crosslink density (shorter distance between crosslink points). It is worth noting that no differences in PIL-CAN Tg values between the first and second heating cycles were found (±1.2 °C), across four replicates of each CAN, indicating not only the ability to reproduce the sample, but also that no change in the bulk thermal properties was observed between heating cycles under the conditions of the experiment (-90 to 120 °C at 2 °C min⁻¹) (Fig. S17†). Both networks were found to exhibit thermal stability up to 275 °C (Fig. S18†) as determined by thermogravimetric analysis (TGA).

Storage modulus (E') was determined for each PIL-CAN (Table 1) using dynamic mechanical analysis (DMA). PIL-CAN-IM exhibited a higher rubbery plateau modulus (1.50 MPa at 80 °C) compared to PIL-CAN-IM2 (0.66 MPa at 80 °C) indicative of a higher crosslink density (Fig. S19†). This is primarily a result of shorter distance between crosslink points in PIL-CAN-IM. Further analysis of the $\tan \delta$ data (Fig. S20†) supports this hypothesis, with PIL-CAN-IM displaying a higher value (49.1 °C).

PILs are single-ion conductors whose conductivity arises from the "hopping" of free counterions among the ions immobilized in the polymer backbone. ⁵⁹ It is well known that most PILs exhibit both Arrhenius and VFT (Vogel–Fulcher–Tamman) behaviour with respect to their ionic conductivities. ^{24–29,37,38,60–62} Arrhenius behaviour, which is commonly observed $\leq T_{\rm g}$, accounts for the thermal "hopping" frequency of ions while non-linear VFT theory accounts for

Table 1 Thermal and mechanical properties of PIL-CANs

	T_{g} (°C)	TGA T _{d5%} (°C)	DMA E' @80 °C (MPa)	tan δ max (°C)
PIL-CAN-IM	12.8	275	1.50	49.1
PIL-CAN-IM2	2.5	296	0.66	33.5

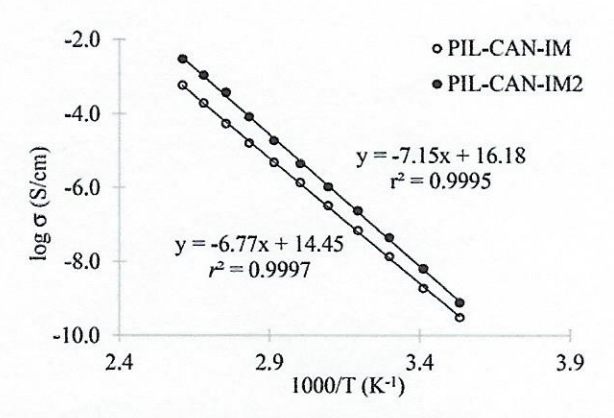
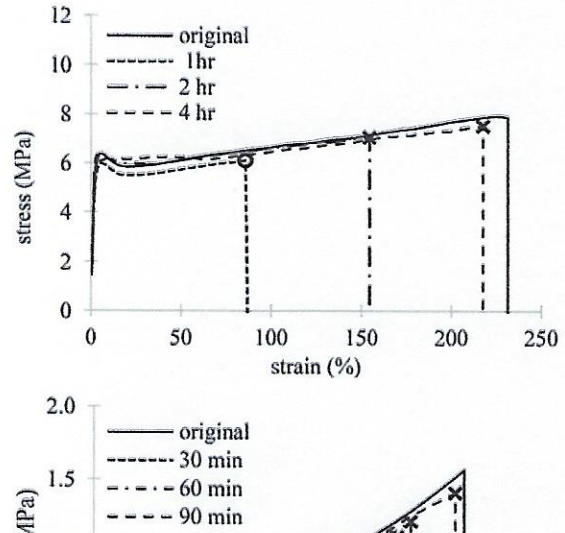


Fig. 2 Temperature-dependent ionic conductivities for PIL-CAN systems. The closed (PIL-CAN-IM2) and open (PIL-CAN-IM) symbols represent experimental data while the solid lines are from Arrhenius fitting.

additional contributions of segmental motion of the polymer and/or polymer relaxation events to the conductivity above $T_{\rm g}$. Temperature-dependent ionic conductivities for the present PIL-CANs were determined under anhydrous conditions using dielectric relaxation spectroscopy (DRS). Conductivity was measured isothermally in 10 °C steps (10-110 °C) using a rheometer with dielectric accessory, over a frequency range of 20.0-106 Hz at a constant axial force. Each sample was allowed to equilibrate at the desired temperature for 45 minutes prior to obtaining data. Both PIL-CANs were found to exhibit only Arrhenius-like behaviour across the temperature range studied ($r^2 > 0.999$), a range which includes temperatures below and above the respective T_g values (Fig. 2). Such a result was unexpected as, with previously studied PIL networks, ionic conductivity typically follows nonlinear VFT behaviour at higher temperatures due to the influence of polymer relaxation events. 48,49,63 Our hypothesis is that, as the temperature approaches $T_{crossover}$ and the network bonds grow more dynamic, the network structure is changing so rapidly relative to any potential chain motions, that ion transport is decoupled from polymer relaxation, leading to Arrhenius-like conductive behaviour. Arrhenius activation energies were found to be 129.6 kJ mol⁻¹ and 136.9 kJ mol⁻¹ for PIL-CAN-IM and PIL-CAN-IM2, respectively.

Recovery of mechanical properties (stress-strain studies) was conducted using a DMA in tensile mode. In short, samples were cut with a razor blade into rectangular pieces, then cut in half perpendicularly. The cut ends were then overlapped by approximately 2 mm, finger pressed, then placed in an oven at a temperature of 105 °C. A TeflonTM weight (200 g) was placed on top to guarantee good contact between the overlapped ends. Samples were periodically removed and the stress and strain at break were determined (Fig. 3). Here, a material is defined as "rehealed" if recovery of >70% of the stress and strain at break is observed with breakage occurring at a new part of the film, away from the reheal junction. PIL-CAN-IM was observed to achieve these conditions at the 2-hour mark while PIL-CAN-IM2 achieved this same result within



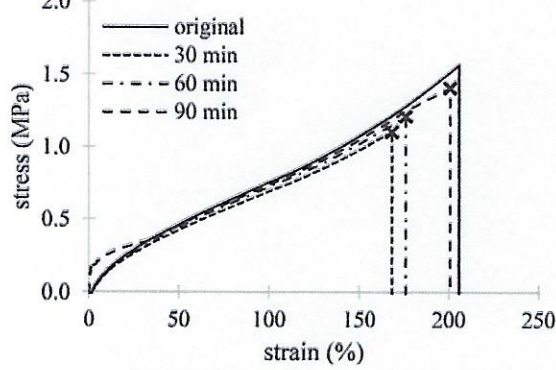


Fig. 3 Stress-strain recovery data for (top) PIL-CAN-IM and (bottom) PIL-CAN-IM2 at 105 °C. Data points marked with an O represent breakage at the original healing point whereas points marked with an X represent breakage at a new point, away from the reheal point.

30 minutes. In fact, after 90 minutes at 105 °C, the overlap spot was nearly absent from the sample (Fig. S27†). A similar observation was made with PIL-CAN-IL at the 4-hour mark. As PIL-CAN-IM was noted to have a higher $T_{\rm crossover}$ temperature (112 νs . 110 °C), it was not surprising that this material took a slightly longer timeframe to exhibit the desired recovery.

An important consideration for a thermoreversible, self-healing material is the ability of the material to resist deformation and creep as a function of time, given a consistent load. Both PIL-CANs were found to exhibit excellent mechanical stability (Fig. S23–S26†). Creep deformation at a constant stress (50% of the respective stress at break) occurred initially for both systems, but plateaued out within 60–90 minutes. Stress relaxation at a constant extension (20% strain) resulted in an even quicker plateau (within 5 minutes). The covalent crosslinking of the Diels–Alder network limits creep and stress relaxation at room temperature, ensuring mechanical stability. Any initial creep or stress relaxation is attributed to the reorganization of ionic bonding/aggregates and other secondary interactions in the networks.

The recovery of sample conductivity via re-healing was determined by passing a current through the sample. Briefly, a 15 mm \times 25 mm \times 0.3 mm rectangular piece of PIL-CAN-IM2 was laid across two planar Cu electrodes and heated to 110 °C while a 500 g weight provided pressure to the top of the

- 11 N. K. Guimard, K. K. Oehlenschlaeger, J. Zhou, S. Hilf, F. G. Schmidt and C. Barner-Kowollik, Macromol. Chem. Phys., 2012, 213, 131.
- 12 C. J. Kloxin and C. N. Bowman, Chem. Soc. Rev., 2013, 42, 7161.
- 13 Y. Yang, X. Ding and M. W. Urban, Prog. Polym. Sci., 2015, 49-50, 34.
- 14 M. K. McBride, B. T. Worrell, T. Brown, L. M. Cox, N. Sowan, C. Wang, M. Podgorski, A. M. Martinez and C. N. Bowman, Annu. Rev. Chem. Biomol. Eng., 2019, 10, 175.
- 15 B. J. Adzima, H. A. Aguirre, C. J. Kloxin, T. F. Scott and C. N. Bowman, *Macromolecules*, 2008, 41, 9112.
- 16 A. Gandini, Prog. Polym. Sci., 2013, 38, 1.
- 17 V. Froidevaux, M. Borne, E. Laborbe, R. Auvergne, A. Gandini and B. Boutevin, RSC Adv., 2015, 5, 37742.
- 18 J. M. Craven, DuPont, US Pat, 3435003, 1969.
- 19 X. Chen, M. A. Dam, K. Ono, A. Mal, H. Shen, S. R. Nutt, K. Sheran and F. Wudl, *Science*, 2002, 295, 1698.
- 20 Y. Imai, H. Itoh, K. Naka and Y. Chujo, *Macromolecules*, 2000, 33, 4343.
- 21 K. Inoue, M. Yamashiro and M. Iji, J. Appl. Polym. Sci., 2009, 112, 876.
- 22 K. Yang, J. C. Grant, P. Lamey, A. Joshi-Imre, B. R. Lund, R. A. Smaldone and W. Voit, *Adv. Funct. Mater.*, 2017, 27, 1700318.
- 23 K. Jin, S. Kim, J. Xu, F. S. Bates and C. J. Ellison, ACS Macro Lett., 2018, 7, 1339.
- 24 D. Mecerreyes, Prog. Polym. Sci., 2011, 36, 1629-1648.
- 25 J. Yuan, D. Mecerreyes and M. Antonetti, Prog. Polym. Sci., 2013, 38, 1009.
- 26 J. Yuan and M. Antonietti, Polymer, 2014, 52, 1469.
- 27 A. S. Shaplov, R. Marcilla and D. Mecerreyes, *Electrochim.*Acta, 2015, 175, 18.
- 28 W. Qian, J. Texter and F. Yan, Chem. Soc. Rev., 2017, 46, 1124.
- 29 N. Matsumi, K. Sugai, M. Miyake and H. Ohno, Macromolecules, 2006, 39, 6924.
- 30 Z. Jia, Q. Lei, F. He, C. Zheng, Y. Liu, X. Zhao and J. Yin, ACS Appl. Polym. Mater., 2019, 1, 2862.
- 31 Y. Gu and T. P. Lodge, Macromolecules, 2011, 44, 1732.
- 32 L. C. Tome, A. S. L. Gouveiz, C. S. R. Freire and D. Mecerreyes, J. Membr. Sci., 2015, 489, 40.
- 33 T. K. Carlisle, E. F. Wiesenauer, G. D. Nicodemus, D. L. Gin and R. D. Noble, *Ind. Eng. Chem. Res.*, 2013, 52, 1023.
- 34 M. G. Cowan, D. L. Gin and R. D. Noble, Acc. Chem. Res., 2016, 49, 724.
- 35 S. Xhang, K. Lee, C. D. Frisbie and T. P. Lodge, Macromolecules, 2011, 44, 940.
- 36 M. Lee, U. H. Choi, D. Salas-de la Cruz, A. Mittal, K. I. Winey, R. H. Colby and H. W. Gibson, Adv. Funct. Mater., 2011, 21, 708.
- 37 S. Takeoka, H. Ohno and E. Tsuchida, Polym. Adv. Technol., 1993, 4, 53.
- 38 S. Dou, S. Zhang, R. J. Klein and R. H. Colby, *Chem. Mater.*, 2006, 18, 4288.

- 39 M. D. Green, D. Salas-de la Cruz, Y. Ye, J. M. Layman, Y A. Elabd, K. I. Winey and T. E. Long, Macromol. Chem. Phys., 2011, 212, 2522.
- 40 D. Salas-de la Cruz, M. D. Green, Y. Ye, Y. A. Elabd and T. E. Long, J. Polym. Sci., Part B: Polym. Phys., 2012, 50, 338.
- 41 U. H. Choi, Y. Ye, D. Salas-de la Cruz, W. Liu, K. I. Winey, Y. A. Elabd, J. Runt and R. H. Colby, *Macromolecules*, 2014, 47, 777.
- 42 C. Iacob, A. Matsumoto, M. Brennan, H. Liu, S. J. Paddison, O. Urakawa, T. Inoue, J. Sangoro and J. Runt, ACS Macro Lett., 2017, 6, 941.
- 43 V. Delhorbe, D. Bresser, H. Mendil-Jakani, P. Rannou, L. Bernard, T. Gutel, S. Lyonnard and L. Picard, Macromolecules, 2017, 50, 4309.
- 44 J. R. Keith, N. J. Rebello, B. J. Cowen and V. Ganesan, ACS Macro Lett., 2019, 8, 387.
- 45 M. Lee, U. H. Choi, D. Salas-de la Cruz, A. Mittal, K. I. Winey, R. H. Colby and H. W. Gibson, Adv. Funct. Mater., 2011, 21, 708.
- 46 S. Kim and K. M. Miller, Polymer, 2012, 53, 5666.
- 47 C. P. Whittington, L. A. Daily and K. M. Miller, *Polymer*, 2014, 55, 3320.
- 48 T. C. Rhoades, J. C. Wistrom, R. D. Johnson and K. M. Miller, *Polymer*, 2016, 100, 1.
- 49 A. F. Bratton, S. Kim, C. J. Ellison and K. M. Miller, *Ind. Eng. Chem. Res.*, 2018, 57, 16526.
- 50 J. Cui, F. Nie, J. Yang, L. Pan, Z. Ma and Y. Li, J. Mater. Chem. A, 2017, 5, 25220.
- 51 P. Guo, H. Zhang, X. Liu and J. Sun, ACS Appl. Mater. Interfaces, 2018, 10, 2105.
- 52 M. M. Obadia, B. P. Mudraboyina, A. Serghei, D. Montarnal and E. Drockenmuller, J. Am. Chem. Soc., 2015, 137, 6078– 6083.
- 53 M. M. Obadia and E. Drockenmuller, Chem. Commun., 2016, 52, 2433-2450.
- 54 P. Chakma, Z. A. Digby, M. P. Shulman, L. R. Kuhn, C. N. Morley, J. L. Sparks and D. Konkolewicz, ACS Macro Lett., 2019, 8, 95–100.
- 55 B. B. Jing and C. M. Evans, J. Am. Chem. Soc., 2019, 141, 18932.
- 56 Y. Cui, Y. Yan and Z. Wang, Macromol. Chem. Phys., 2013, 214, 470.
- 57 J. Bara, Ind. Eng. Chem. Res., 2011, 50, 13614.
- 58 K. Sugane, N. Kumai, Y. Yoshioka, A. Shibita and M. Shibata, *Polymer*, 2017, 124, 20.
- 59 J. R. Keith, N. J. Rebello, B. J. Cowen and V. Ganesan, ACS Macro Lett., 2019, 8, 387.
- 60 H. Chen, J. Choi, D. Salas-de la Cruz, K. I. Winey and Y. A. Elabd, Macromolecules, 2009, 42, 4809.
- 61 D. Fragiadakis, S. Dou, R. H. Colby and J. Runt, *J. Chem. Phys.*, 2009, **130**, 064907.
- 62 K. Nakamura, T. Saiwaki and K. Fukao, *Macromolecules*, 2010, 43, 6092.
- 63 C. A. Tracy, A. M. Adler, A. Nguyen, R. D. Johnson and K. M. Miller, ACS Omega, 2018, 3, 13442.